

# Thermal Conductivity of Plasma-Sprayed Aluminum Oxide—Multiwalled Carbon Nanotube Composites

Srinivas R. Bakshi, Kantesh Balani, and Arvind Agarwal†

Department of Mechanical and Materials Engineering, Florida International University, Miami, Florida

**Aluminum oxide nanocomposites reinforced with multiwalled carbon nanotubes (MWNT) were prepared by atmospheric plasma spraying of blended and spray-dried powders. Thermal conductivity was measured using the laser flash technique for temperatures between 25° and 300°C. An aluminum oxide—4 wt% MWNT nanocomposite prepared from the blended powder showed the highest conductivity, followed by aluminum oxide without nanotubes, 8 and 4 wt% MWNT composite prepared from spray-dried powder in that order. The thermal conductivity values obtained are rationalized taking into account the crystallite size, porosity, MWNT content, microstructure, and the interfaces and metastable  $\gamma$ -Al<sub>2</sub>O<sub>3</sub> content present in the nanocomposite.**

## I. Introduction

Thermal conductivity is an important physical property, which is required in modeling heat transfer through solids and structures. It has also been used as a quality control parameter in the production and performance of nuclear fuels<sup>1</sup> and thermal barrier coatings.<sup>2</sup> Carbon nanotubes have shown excellent mechanical, thermal, and electrical properties due to which they have been proposed for a myriad number of applications.<sup>3</sup> Multiwalled carbon nanotubes (MWNT) have also shown<sup>4</sup> very high thermal conductivities in excess of 3000 W·(m·K)<sup>-1</sup>. Hence, they serve as a first choice of materials as fillers for thermal conductivity enhancement in thermal management materials. The thermal conductivity of dense aluminum oxide has been reported<sup>5</sup> to be between 27 and 35 W·(m·K)<sup>-1</sup>. In our previous work,<sup>6</sup> it has been shown that addition of carbon nanotubes to aluminum oxide resulted in a 43% increase in the fracture toughness. Addition of MWNT is also expected to increase the thermal conductivity of the composites, which is beneficial for many applications like electronic packaging. It is generally difficult to predict the thermal conductivity of plasma-sprayed coatings because of its complicated microstructure, which consists of splats, porosity, and interfaces. The goal of this paper is to study the thermal conductivity of plasma-sprayed aluminum oxide—MWNT nanocomposites and rationalize them by taking into account the crystallite size, porosity, MWNT content, matrix microstructure, interfaces, and metastable  $\gamma$ -Al<sub>2</sub>O<sub>3</sub> content present in the coatings.

## II. Experimental Procedure

### (1) Plasma Spraying

The samples were fabricated using DC arc plasma spraying with a Praxair SG-100 gun (Praxair Inc., Danbury, CT). The powders were fed internally into the plasma using argon as a carrier gas. Four types of powders were sprayed. They are (a) a spray-dried nanoaluminum oxide (referred to as nano-Al<sub>2</sub>O<sub>3</sub> hereafter), (b) a

spray-dried nanoaluminum oxide blended with 4 wt% MWNT (referred to as Al<sub>2</sub>O<sub>3</sub>—4 wt% MWNT blended hereafter), (c) a spray-dried nanoaluminum oxide 4 wt% MWNT mixture (referred to as Al<sub>2</sub>O<sub>3</sub>—4 wt% MWNT spray dried hereafter), and (d) a spray-dried nanoaluminum oxide 8 wt% MWNT mixture (referred to as Al<sub>2</sub>O<sub>3</sub>—8 wt% MWNT spray dried hereafter). Coatings of thickness between 0.5 and 1 mm were sprayed onto a mild steel substrate. The details of the plasma spraying and the microstructure of the coatings are given elsewhere.<sup>6</sup> Carbon nanotubes were found to be well distributed in the partially molten regions and were also found in the intersplat and inter-particle regions.<sup>6</sup> It was also seen that the nanotubes were coated well with Al<sub>2</sub>O<sub>3</sub>, indicating wetting and better interfacial heat transfer between the two. Undamaged CNTs in the plasma-sprayed coatings were confirmed from scanning electron microscope (SEM, JEOL JSM-6330F, JEOL USA Inc., Peabody, MA) observation of fracture surfaces,<sup>6</sup> micro-Raman spectroscopy,<sup>6</sup> and high-resolution transmission electron microscopy (HRTEM, FEI Tecnai F30, FEI Company, Hillsboro, OR).

### (2) Thermal Conductivity Measurement

To fabricate samples for thermal conductivity, the substrate with coating was cut into a 10 mm × 10 mm piece with a low-speed diamond saw (Buehler Isomet 11-1180, Buehler Ltd., Lake Bluff, IL). The diamond saw was used to cut through the substrate. The thin layer of mild steel attached to the coating was then removed by dissolving in nitric acid. Thus, free-standing samples of 10 mm × 10 mm area and 0.5–1-mm thickness were prepared. The bulk density of the samples was measured by the water displacement method using the Archimedes principle. Thermal diffusivity was measured using a Holometrix Micromet-300 Thermal Diffusivity Instrument (Metrisa Inc., Bedford, MA) by the pulse method for a number of temperatures between 25° and 300°C. The thermal diffusivity values were corrected for radiation heat losses using Cowan's method.<sup>7</sup> The nano-Al<sub>2</sub>O<sub>3</sub> sample was coated with carbon using a carbon spray, to make it opaque to the laser radiation, and then the edges were ground to ensure that the carbon layer was only at the top and bottom surfaces. The MWNT-containing nanocomposites did not require any carbon coating as they were already opaque to the laser radiation. The error in the measured values of thermal diffusivity was within ±3%. The specific heat capacity of aluminum oxide was taken from the thermodynamic databank FactSage 5.0.<sup>8</sup> The specific heat of carbon nanotubes was taken to be the same as that of graphite and was also obtained from FactSage 5.0. Masarapu *et al.*<sup>9</sup> determined the specific heat capacity of aligned multiwalled carbon nanotubes and found it to be similar to that of graphite. The specific heat capacities of the 4 and 8 wt% MWNT composites were calculated using the Neumann–Kopp additive rule. Finally, the thermal conductivity was calculated from the following equation:

$$k = \alpha \cdot \rho \cdot C_p \quad (1)$$

Here,  $k$  is the thermal conductivity,  $\alpha$  is the measured value of thermal diffusivity,  $\rho$  is the bulk density, and  $C_p$  is the specific heat capacity.

K. Watari—contributing editor

Manuscript No. 23313. Received June 6, 2007; approved August 19, 2007.

†Author to whom correspondence should be addressed. e-mail: agarwala@fiu.edu

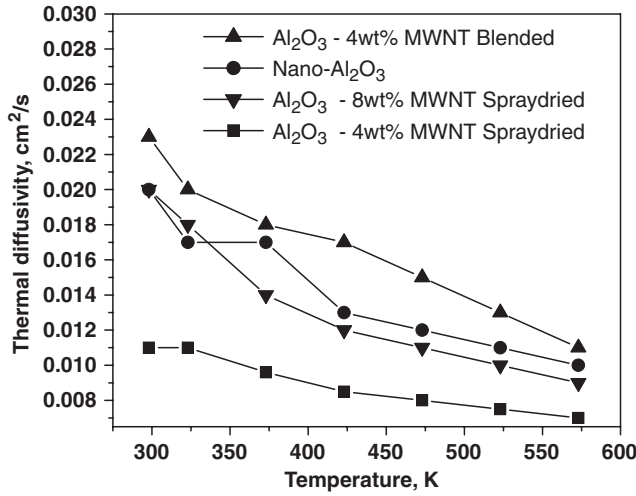


Fig. 1. Variation of thermal diffusivity with temperature.

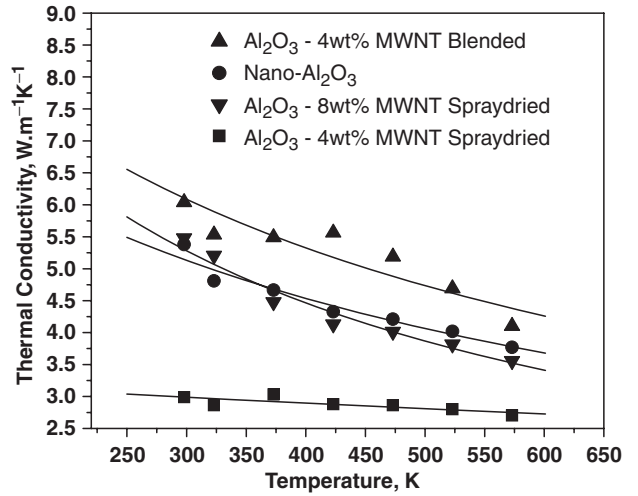


Fig. 2. Variation of thermal conductivity with temperature.

III. Results and Discussion

(1) Variation of Thermal Properties with Temperature

Figure 1 shows the variation of the thermal diffusivity of the nanocomposites with temperature. Similar to all dielectric materials, the thermal diffusivity decreases with an increase in the temperature. The Al<sub>2</sub>O<sub>3</sub>–4 wt% MWNT blended nanocomposite has the highest thermal diffusivity, while the Al<sub>2</sub>O<sub>3</sub>–4 wt% MWNT spray-dried nanocomposite has the lowest. The variation of the thermal conductivity has been plotted in Fig. 2. The solid curves in the figure represent the least square fit for the data with an equation of the type  $(A+BT)^{-1}$  where  $A$  and  $B$  are constants and  $T$  is the absolute temperature. The thermal conductivity decreases with an increase in temperature endorsing the phonon mechanism of heat conduction.

It is observed that the Al<sub>2</sub>O<sub>3</sub>–4 wt% MWNT-blended nanocomposite coating has the highest thermal conductivity. For the Al<sub>2</sub>O<sub>3</sub>–MWNT nanocomposite synthesized from spray-dried powder, the thermal conductivity increases with the increase in the MWNT content.

The thermal conductivities of the nano-Al<sub>2</sub>O<sub>3</sub> and the Al<sub>2</sub>O<sub>3</sub>–8 wt% MWNT spray-dried nanocomposite are almost similar. The thermal conductivity is affected by many factors like the crystallite boundaries, porosity, carbon nanotube content, interphase boundaries, and phase content. It is a complex function of the above features. In the following analysis, the thermal conductivity will be considered to be influenced by the crystallite size, porosity, and the MWNT content. This can be expressed by the following equation:

$$k_c = f_1(r) \times f_2(f_p) \times f_3(f_{MWNT}) \tag{2}$$

where  $k_c$  is the overall thermal conductivity of the composite,  $r$  the crystallite size of  $\alpha$ -Al<sub>2</sub>O<sub>3</sub>,  $f_p$  the volume fraction of porosity present in the coatings,  $f_{MWNT}$  is the volume fraction of MWNT present in the coatings, and  $f_1$ ,  $f_2$ , and  $f_3$  denote functions.

(2) Effect of Crystallite Size

Thermal resistance at the crystallite boundaries can lead to lowering of thermal conductivity. The thermal conductivity of a crystal with a known crystallite size can be expressed according to the relation<sup>10</sup>

$$\frac{1}{k_{mn}} = \frac{1}{k_m} + n \cdot R_{bound} \tag{3}$$

where  $n$  is the number of crystallites per unit length,  $k_m$  the theoretical or the single-crystal thermal conductivity of Al<sub>2</sub>O<sub>3</sub>,  $k_{mn}$  the thermal conductivity of  $\alpha$ -Al<sub>2</sub>O<sub>3</sub> with nanocrystalline grains, and  $R$  is the boundary thermal resistance or the Kapitza resistance. The crystallite size and phase content in the coatings have been tabulated in Table I. The crystallite size of the phases in the initial powders and coatings was determined using the peak width of the XRD curves of the samples and sapphire reference. It is to be noted that the powder contains a 100%  $\alpha$ -Al<sub>2</sub>O<sub>3</sub> phase. Also, we see that the crystallite size of  $\alpha$ -Al<sub>2</sub>O<sub>3</sub> in the coatings is more than that in the powders.

This is due to the grain coalescence and growth during plasma spraying. In the Al<sub>2</sub>O<sub>3</sub>–4 wt% MWNT-blended sample, all the nanotubes reside on the surface of the spray-dried particle as compared with the Al<sub>2</sub>O<sub>3</sub>–4 wt% MWNT spray-dried powder. Hence, there is more absorption and retention of heat and consequently more coarsening in case of the Al<sub>2</sub>O<sub>3</sub>–4 wt% MWNT-blended coating. This also explains the increase in crystallite size with the increase in MWNT percent. Yang *et al.*<sup>11</sup> have measured the temperature dependence of the crystallite boundary resistance and have shown that they are efficient in reducing the thermal conductivity of YSZ. They found the Kapitza resistance to be between  $0.4 \times 10^{-8}$  and  $2 \times 10^{-8} \text{ m}^2 \cdot (\text{W} \cdot \text{K})^{-1}$ . Crystallite size and thermal conductivity values of  $\alpha$ -Al<sub>2</sub>O<sub>3</sub> were used for the computation because there are no data available for the thermal properties of  $\gamma$ -Al<sub>2</sub>O<sub>3</sub>. The value for the boundary resistance was taken to be equal to  $1 \times 10^{-8}$

Table I. Phase Content and Crystallite Size of the Powders and the Coatings

Crystallite size and phase content	Powder	Coating			
	$\alpha$ -Al <sub>2</sub> O <sub>3</sub> crystallite size (nm)	$\alpha$ -Al <sub>2</sub> O <sub>3</sub> crystallite size (nm)	$\alpha$ -Al <sub>2</sub> O <sub>3</sub> content (%)	$\gamma$ -Al <sub>2</sub> O <sub>3</sub> crystallite size (nm)	$\gamma$ -Al <sub>2</sub> O <sub>3</sub> content (%)
Nano-Al <sub>2</sub> O <sub>3</sub>	44	55	77	22	23
Al <sub>2</sub> O <sub>3</sub> –4 wt% MWNT blended	46	95	68	13	32
Al <sub>2</sub> O <sub>3</sub> –4 wt% MWNT spray dried	45	73	82	15	18
Al <sub>2</sub> O <sub>3</sub> –8 wt% MWNT spray dried	43	76	75	21	25

Amount and crystallite size of  $\alpha$  and  $\gamma$  phase of aluminum oxide present in the coatings as measured from the area under peaks and peak broadening in XRD patterns of the coating. Note the large crystallite size of  $\alpha$  phase in case of Al<sub>2</sub>O<sub>3</sub>–4 wt% MWNT Blended coating.

**Table II. Calculated Values of Thermal Conductivity Based on Crystallite Size of  $\alpha$ -Phase**

Sample	Crystallite size of $\alpha$ -phase (nm)	Number of crystallites per unit length ( $\text{m}^{-1}$ )	Calculated thermal conductivity, $k_{mn}$ ( $\text{W} \cdot (\text{m} \cdot \text{K})^{-1}$ )
Nano- $\text{Al}_2\text{O}_3$	55	1 81 81 800	4.6
$\text{Al}_2\text{O}_3$ -4 wt% MWNT blended	95	1 05 26 300	7.2
$\text{Al}_2\text{O}_3$ -4 wt% MWNT spray dried	73	1 36 98 600	5.9
$\text{Al}_2\text{O}_3$ -8 wt% MWNT spray dried	76	1 31 57 900	6.1

$k_{mn}$ —Thermal conductivity of 100 percent dense matrix with nanocrystalline structure. Effect of crystallite size and hence amount crystallite boundary on the thermal conductivity. It is the main factor in reducing the thermal conductivity of the coatings and the main reason for the higher thermal conductivity of  $\text{Al}_2\text{O}_3$ -4wt% MWNT-blended coating.

$\text{m}^2 \cdot (\text{W} \cdot \text{K})^{-1}$ , which is the average of that calculated by Yang *et al.*<sup>11</sup> and that has also been used by Poulter *et al.*<sup>10</sup> for alumina. The value of  $k_m$  was taken to be  $30 \text{ W} \cdot (\text{m} \cdot \text{K})^{-1}$ . The calculated values of the thermal conductivity have been tabulated in Table II.

It can be seen that the crystallite size of the  $\text{Al}_2\text{O}_3$ -4 wt% MWNT-blended coating is the highest, and it is expected to have a higher conductivity due to the presence of lower number of interfaces. This is the main reason for the high thermal conductivity of the  $\text{Al}_2\text{O}_3$ -4 wt% MWNT-blended coating. The values tabulated in Table II will be used as the thermal conductivity values for the 100% dense samples ( $k_{mn}$ ) in all calculations that follow.

### (3) Effect of Porosity

The porosity content present in the plasma-sprayed nanocomposites has been tabulated in Table III. Porosities scatter phonons and hence the more the porosity, the lower the conductivity. Also, the porosities are filled with air, which has poor conductivity. One reason for the higher values of the thermal conductivity of the  $\text{Al}_2\text{O}_3$ -8 wt% MWNT spray-dried coating as compared with the  $\text{Al}_2\text{O}_3$ -4 wt% MWNT spray-dried coating is its lower porosity content. As mentioned earlier, the thermal conductivity of aluminum oxide has been reported<sup>5</sup> to be between  $27$  and  $35 \text{ W} \cdot (\text{m} \cdot \text{K})^{-1}$  at room temperature, which is very high compared with the values obtained in this work. The samples in the above-mentioned work were all hot-pressed or sintered and had an equiaxed microstructure with a comparatively coarser grain size than our coatings. Various relationships have been proposed for the porosity dependence of thermal conductivity based on the shape and distribution of the pores, especially in the context of nuclear fuels.<sup>12-15</sup>

The usual porosity relations that hold true for sintered or hot-pressed compacts do not hold true for plasma-sprayed coatings. The thermal conductivities of plasma-sprayed aluminum oxide and zirconium oxide coatings are much smaller than those predicted by these relationships.<sup>16-17</sup> This is due to the fact that the above relations are derived considering the pores to be spherical or prolate or oblate spheroids. Plasma-sprayed coatings have a lamellar microstructure with pores in between the lamellae. The pores are like very thin disks and because they are all aligned parallel to the thickness of the coating, they reduce the transverse thermal conductivity drastically. The formulas for the

thermal conductivity of the nanocrystalline matrix with pores according to various models are listed below:

Landauer<sup>18</sup>

$$k_{mnp} = \frac{1}{4} \left[ k_p(3f_p - 1) + k_{mn}(2 - 3f_p) + \left\{ [k_p(3f_p - 1) + k_{mn}(2 - 3f_p)]^2 + 8k_{mn}k_p \right\}^{1/2} \right] \quad (4)$$

Meredith and Tobias<sup>19</sup>

$$\frac{k_{mnp}}{k_{mn}} = \left[ \frac{2 - f_p}{2 + (W - 1)f_p} \right] \left[ \frac{2(1 - f_p)}{2(1 - f_p) + Wf_p} \right] \quad (5)$$

where  $W = \frac{1}{3} \left( \frac{1}{2F} + \frac{2}{(1-F)} \right)$ ,  $F$  is the shape factor, which is 0.1 for lamellar pores.

Shafiro and Kachanov<sup>20</sup>

$$\frac{k_{mnp}}{k_{mn}} = 1 - \left( \frac{2f_p}{\pi} \right) \left( \frac{d}{t} \right) \quad (6)$$

where  $f_p$  is the fractional porosity and  $d/t$  is the aspect ratio of the lamellar pores, which will be taken as 5 here. Here,  $k_{mnp}$  refers to the thermal conductivity of the nanocrystalline matrix containing the pores and  $k_p$  refers to the thermal conductivity of the pore. This value of the aspect ratio is taken in accordance to that observed by Wang *et al.*<sup>21</sup> The values of thermal conductivity of the porous coatings were calculated based on the porosity relations mentioned above by taking the value of  $k_{mn}$  from Table II and porosity values from Table III and  $k_p = 0.4 \text{ W} \cdot (\text{m} \cdot \text{K})^{-1}$ , and has been tabulated in Table IV below.

It can be observed that the values of the thermal conductivity calculated in this manner are close to that measured experimentally for the  $\text{Al}_2\text{O}_3$ -4 wt% MWNT blended and the  $\text{Al}_2\text{O}_3$ -8 wt% MWNT spray-dried coatings. The nano- $\text{Al}_2\text{O}_3$  coating exhibits a larger conductivity compared with the calculated one, which may be due to the smaller value of Kapitza resistance for the interfaces of  $\alpha$ - $\text{Al}_2\text{O}_3$  crystallites. The effect of addition of carbon nanotubes has not been taken into account yet. The addition of carbon nanotubes will increase the computed values of the thermal conductivities of the composites. The thermal conductivity of plasma-sprayed zirconium oxide and aluminum oxide has been shown to be very low compared with the thermal conductivity of fully dense compacts produced by other methods.<sup>16,17,21,22</sup> Our values for aluminum oxide are in agreement with those reported by Kulkarni *et al.*<sup>22</sup> McPherson<sup>23</sup> has provided a model for thermal conductivity of plasma-sprayed coatings, considering that there are only a few regions of good contact between the lamella and existence of planar pores, which are essentially nonconducting at low temperatures. According to the model, the ratio of the thermal resistivity of the coating ( $R_c$ ) and a fully dense bulk material ( $R_b$ ) is given by

$$\frac{R_c}{R_b} = \frac{\pi a}{2f\delta} \quad (7)$$

where “ $2a$ ” is the mean radius of the circular regions of contact between the splats,  $f$  is the mean fraction of the total area in true contact in any plane parallel to the coating surface, and  $\delta$  is the

**Table III. Density and Porosity Fraction Present in the Coatings**

Coating	Density $\text{g}/\text{cm}^3$	Porosity %
Nano- $\text{Al}_2\text{O}_3$	3.47	13
$\text{Al}_2\text{O}_3$ -4wt% MWNT blended	3.40	12.8
$\text{Al}_2\text{O}_3$ -4wt% MWNT spray dried	3.52	9.8
$\text{Al}_2\text{O}_3$ -8wt% MWNT spray dried	3.53	6

Note that the fractional porosity reduces of the coatings formed from the spray-dried powders reduces with increase in CNT content. Thermal conductivity of the  $\text{Al}_2\text{O}_3$ -4wt% MWNT blended coating is highest irrespective of its higher porosity.

**Table IV. Calculated Thermal Conductivity of the Composites Based on the Porosity Relations at 298 K**

Sample	Porosity fraction	Measured $k$ at 298 K, (W · (m · K) <sup>-1</sup> )	Calculated $k_{mmp}$ at 298 K (W · (m · K) <sup>-1</sup> )		
			Landauer Model	Meredith and Tobias Model	Kachanov Model
Nano-Al <sub>2</sub> O <sub>3</sub> coating	0.13	5.4	3.8	3.3	2.7
Al <sub>2</sub> O <sub>3</sub> -4wt% MWNT blended	0.128	6.0	5.9	5.3	4.3
Al <sub>2</sub> O <sub>3</sub> -4wt% MWNT spray dried	0.098	3.0	5.1	4.6	4.0
Al <sub>2</sub> O <sub>3</sub> -8wt% MWNT spray dried	0.06	5.5	5.6	5.3	4.9

$k_{mmp}$  is the computed value of the thermal conductivity of the nanocrystalline Al<sub>2</sub>O<sub>3</sub> matrix containing pores. The Meredith and Tobias model, which takes into account the pore shape, gives values close to the observed values. These values are used for further calculations.

thickness of the lamella or splats. From transmission electron microscope (TEM) images of the coatings, it was found that “ $2a$ ” is comparable with “ $r$ ” and the value of “ $f$ ” can be taken to be around 0.2 from the fact that the values of elastic modulus of the coatings are around 0.2 times the theoretical values. Using these values,  $R_c/R_b$  is calculated to be around 4. This means that the thermal conductivity of plasma-sprayed coatings can be as low as 0.25 times the bulk value. Hence, the model predicts the observed values quite well, qualitatively.

#### (4) Effect of MWNT Addition

Improvements in thermal conductivity have been reported due to the addition of nanotubes.<sup>24,25</sup> Recently, Sivakumar *et al.*<sup>26</sup> have reported a 70% increase in thermal conductivity of SiO<sub>2</sub> due to the addition of 10 vol.% of MWNT. This increase is very low compared with the calculated values obtained from a simple rule of mixtures.

This indicates that the interfacial thermal resistance plays an important role in determining the effective thermal conductivity.

Conventional models of thermal conductivity of composites predict a large value for the thermal conductivity of MWNT composites and this has led to the development of new models based on the Effective Medium Approach (EMA) of Maxwell–Garnett.<sup>27–29</sup> These are summarized below in Table V.

Here,  $k_e$  is the effective thermal conductivity of the composite,  $k_{mmp}$  is the thermal conductivity of the matrix taken from Meredith and Tobias values of Table III,  $k_c$  is the MWNT thermal conductivity (3000 W · (m · K)<sup>-1</sup>),  $f$  is the MWNT volume fraction,  $\alpha = k_c/k_{mmp}$ , and  $a_k$  is the so-called Kapitza radius, which is given as  $a_k = R_k k_m$  where  $R_k$  is the Kapitza resistance or the thermal boundary resistance. The Kapitza radius is assumed to be 15 nm here. The MWNT used are 40–70 nm in diameter and 0.5–2  $\mu$ m in length. The MWNT volume fraction  $f_{MWNT}$  is equal to 6.6% and 12.4% for the 4 and 8 wt%, composite, respectively. It can be seen that the value obtained from the rule of mixture formula is quite large. It is seen from Table V that the values obtained from these EMA models are larger than the observed values by a factor of 2–3. Huxtable *et al.*<sup>30</sup> have shown that an exceptionally small interfacial heat conductance

**Table V. Calculated Thermal Conductivity Values at 298 K for Different MWNT Content**

Reference	Model formulation	Calculated $k_e$ at 298 K (W · (m · K) <sup>-1</sup> )		
		Al <sub>2</sub> O <sub>3</sub> -4wt% MWNT blended	Al <sub>2</sub> O <sub>3</sub> -4wt% MWNT spray dried	Al <sub>2</sub> O <sub>3</sub> -8wt% MWNT spray dried
Rule of mixtures <sup>26</sup>	$\frac{k_e}{k_{mmp}} = 1 + \frac{f_{MWNT} k_c}{3k_{mmp}}$	77	71	129
Nan <i>et al.</i> <sup>29</sup>	$\frac{k_e}{k_{mmp}} = \frac{3 + f_{MWNT}(\beta_x + \beta_z)}{3 - 2\beta_x},$ $\beta_x = \frac{2(k_{11}^c - k_{mmp})}{k_{11}^c + k_{mmp}}, \quad \beta_z = \frac{k_{33}^c}{k_{mmp}} - 1$ $k_{11}^c = \frac{k_c}{1 + \frac{2a_k}{d} \frac{k_c}{k_{mmp}}}, \quad k_{33}^c = \frac{k_c}{1 + \frac{2a_k}{L} \frac{k_c}{k_{mmp}}}$	11	10	15
Xue <sup>28</sup> with good dispersion	$\frac{k_e}{k_{mmp}} = \frac{1 - f_{MWNT} + (4f_{MWNT}/\pi)\sqrt{k_c/k_{mmp}} \times \tan^{-1}(\pi/4\sqrt{k_c/k_{mmp}})}{1 - f_{MWNT} + (4f_{MWNT}/\pi)\sqrt{k_{mmp}/k_c} \times \tan^{-1}(\pi/4\sqrt{k_c/k_{mmp}})}$	22	21	39
Xue <sup>28</sup> with poor dispersion	$\frac{k_e}{k_{mmp}} = \frac{1 - f_{MWNT} + 2f_{MWNT} \frac{k_c}{k_c - k_{mmp}} \ln \frac{k_c + k_{mmp}}{2k_{mmp}}}{1 - f_{MWNT} + 2f_{MWNT} \frac{k_{mmp}}{k_c - k_{mmp}} \ln \frac{k_c + k_{mmp}}{2k_{mmp}}}$	10	8	14

Thermal conductivities are ( $k_c$ : CNT composite,  $k_c$ : multiwalled CNT,  $k_{mmp}$ : nanocrystalline matrix with porosity). Models based on EMA approach are used to calculate thermal conductivity of CNT composites.

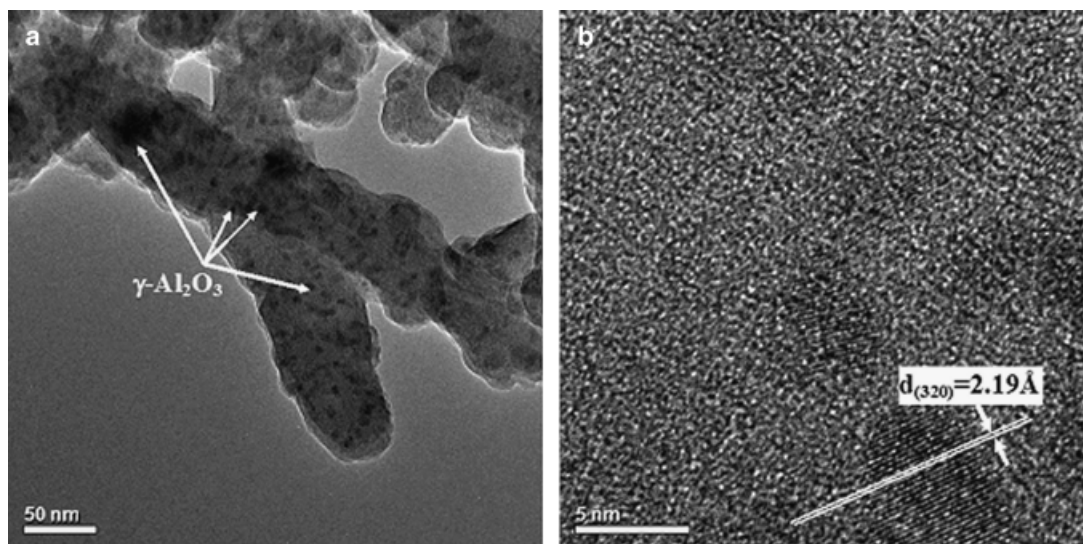


**Fig. 3.** Transmission electron microscopic image of the (a)  $\text{Al}_2\text{O}_3$ —8 wt% multiwalled carbon nanotubes (MWNT) spray dried coating showing the  $\gamma\text{-Al}_2\text{O}_3$  nucleated on MWNT, and (b) HRTEM image of the nanotube surface showing a  $\gamma\text{-Al}_2\text{O}_3$  precipitate.

of  $12 \text{ MW} \cdot (\text{m} \cdot \text{K})^{-1} \cdot \text{K}$  limits the enhancement of the thermal conductivity of CNT composites. Shenogina *et al.*<sup>31</sup> performed FEM calculations and found that as the distance between the two nanotubes approached zero, the rate of heat flow in the composite increased only marginally, indicating a possible lack of thermal percolation in carbon nanotube composites. Zhan *et al.*<sup>32</sup> have observed thermal conductivity of aluminum oxide—SWNT composites as compared with aluminum oxide prepared by spark plasma sintering. They also found that the thermal conductivity reduced with increasing vol.% of SWNT. They had attributed this to the lower thermal conductivity of SWNT bundles and possibly the high thermal resistivity of the SWNT— $\text{Al}_2\text{O}_3$  interface. However, there could be many reasons for the observed lower values of the thermal conductivity than tabulated in Table IV, which will be discussed below.

(A) *Effect of Intersplat Thermal Resistance:* It is known that during plasma spraying, the powder feedstock is introduced into the plasma where particles become heated. A molten/semi-molten particle accelerates and strikes the substrate at high velocities<sup>6</sup> of  $\sim 200 \text{ m/s}$  and forms a splat (as measured using in-flight particle diagnostic sensor Accuraspray G3, Tecnar Automation LTEE, St. Bruno, QC, Canada). Hence, the nanocomposite has a layered morphology with interlamellar pores, intersplat interfaces, partially molten particles, and cracks due to thermal stress. Ravichandran *et al.*<sup>17</sup> have obtained values of thermal conductivity of plasma-sprayed alumina with 19% porosity as low as  $1/10$  ( $\sim 3 \text{ W} \cdot (\text{m} \cdot \text{K})^{-1}$  at room temperature) of the theoretical value. According to their simple interfacial thermal resistance model,<sup>21</sup> the effective value of thermal conductivity of a layered splat-like microstructure is given by

$$k_{\text{eff}} = \frac{L}{\frac{n\delta}{k_m} + \frac{n-1}{h_i}} \quad (8)$$

where  $L$  is the total thickness of the coating,  $n$  the number of splats making up the coating,  $\delta$  the average splat thickness,  $k_m$  the thermal conductivity of the bulk material, and  $h_i$  is the interfacial heat transfer coefficient. Hence, for a coating of aluminum oxide made of 100 splats of thickness  $1 \mu\text{m}$  each and assuming  $h_i$  to be  $10^6 \text{ W} \cdot (\text{m} \cdot \text{K})^{-1}$  and  $k_m$  to be  $30 \text{ W} \cdot (\text{m} \cdot \text{K})^{-1}$ , one gets the  $k_{\text{eff}}$  value as low as  $1 \text{ W} \cdot (\text{m} \cdot \text{K})^{-1}$ . So it is seen that interfacial resistance plays a significant role in reducing the thermal conductivity value. The value of the interfacial heat transfer coefficient will depend on many parameters including the area of contact, contact pressure due to residual stresses, impurity segregation, and gas pressure in the voids,

which are all dependent on many processing parameters. Hence it is not possible to assign a reasonable value or predict the value of the heat transfer coefficient at the interfaces. The MWNT distribution and morphology between the splats will also influence the interfacial conductance.

(B) *Effect of  $\gamma\text{-Al}_2\text{O}_3$  Formation:* It is well known that during plasma spraying, metastable  $\gamma\text{-Al}_2\text{O}_3$  forms during plasma spraying.<sup>33,34</sup> Guilemany *et al.*<sup>34</sup> have found that plasma-sprayed  $\alpha\text{-Al}_2\text{O}_3$  coatings contain between 17% and 23% of  $\alpha\text{-Al}_2\text{O}_3$  and the rest  $\gamma\text{-Al}_2\text{O}_3$ . The phase resulting from re-solidification of aluminum oxide is always the metastable phase  $\gamma\text{-Al}_2\text{O}_3$ . Figure 3 shows a TEM micrograph of the  $\text{Al}_2\text{O}_3$ —8 wt% MWNT spray-dried coating. It can be seen that CNT act as nucleation sites for  $\gamma\text{-Al}_2\text{O}_3$ . As stated, previously in the  $\text{Al}_2\text{O}_3$ —4 wt% MWNT-blended powder, the nanotubes reside on the surface and this leads to more absorption and retention of heat and consequently a higher degree of melting compared with the  $\text{Al}_2\text{O}_3$ —4 wt% MWNT spray dried and the  $\text{Al}_2\text{O}_3$ —8 wt% MWNT spray-dried coating. This, combined with the fact that  $\gamma\text{-Al}_2\text{O}_3$  nucleates on MWNT, explains the higher amount of  $\gamma\text{-Al}_2\text{O}_3$  in the  $\text{Al}_2\text{O}_3$ —4 wt% MWNT-blended coating. The more the amount of  $\gamma\text{-Al}_2\text{O}_3$ , the more the interfacial area between  $\gamma\text{-Al}_2\text{O}_3$  and  $\alpha\text{-Al}_2\text{O}_3$ , which will provide an additional interfacial resistance term and will reduce the thermal conductivity. The higher value of the thermal conductivity of the  $\text{Al}_2\text{O}_3$ —4 wt% MWNT-blended coating might be due to the overwhelming effect of an increase in the crystallite size of  $\alpha\text{-Al}_2\text{O}_3$ .

The modeling of the effect of the  $\gamma\text{-Al}_2\text{O}_3$  content on the thermal conductivity will require knowledge of the interface resistance and will involve the distribution and orientation of the  $\gamma$  and  $\alpha$  interfaces and a value of thermal conductivity for the  $\gamma\text{-Al}_2\text{O}_3$  phase that is not available in the literature because of its metastable nature. Also the  $\gamma\text{-Al}_2\text{O}_3$  content and distribution is a function of many processing parameters and is difficult to quantify.

#### IV. Conclusions

The thermal conductivity of plasma-sprayed aluminum oxide blended with 4 wt% MWNT was higher than the coatings obtained from spray-dried powders containing 4 and 8 wt% MWNT. The thermal conductivity increases with an increase in the MWNT content. The crystallite size has a strong effect in reducing the thermal conductivity of the coatings. The addition of MWNT does not increase the values of the thermal conductivity significantly as predicted by the models based on the

Effective Medium Approach. The measured thermal conductivity values of the plasma-sprayed coatings are two to three times lower than that calculated by taking into consideration the boundary resistance. The lower thermal conductivity of the  $Al_2O_3$ -MWNT composite coatings can be ascribed to the inter-splat thermal resistance, which is difficult to quantify. MWNT acts as nucleation sites for  $\gamma$ - $Al_2O_3$  formation and the  $\gamma$ - $Al_2O_3$  serves as phonon-scattering centers, further reducing the thermal conductivity. It is challenging to quantify the effect of the crystallite size and content of  $\gamma$ - $Al_2O_3$  due to the unavailability of data on the physical properties and the complexity of the distribution of  $\gamma$ - $Al_2O_3$ .

### Acknowledgments

The authors would like to acknowledge the research funding from the Office of Naval Research (N00014-05-1-0398) for carrying out this research. One of the authors (S. R. Bakshi) would like to acknowledge Presidential Enhanced Assistantship from FIU and National Science Foundation (DMI-0547178) for funding. Kantesh Balani acknowledges Dissertation Year Fellowship from FIU.

### References

- <sup>1</sup>D. G. Martin, "A Re-appraisal of the Thermal Conductivity of  $UO_2$  and Mixed (U, Pu) Oxide Fuels," *J. Nucl. Mater.*, **110**, 73–94 (1982).
- <sup>2</sup>D. R. Clarke and S. R. Phillpot, "Materials," *Mater. Today*, **8**, 22–9 (2005).
- <sup>3</sup>R. H. Baugman, A. A. Zakhidov, and W. A. de Heer, "Carbon Nanotube—The Route Towards Applications," *Science*, **297**, 787–92 (2002).
- <sup>4</sup>P. Kim, L. Shi, A. Majumdar, and P. L. McEuen, "Thermal Transport Measurements of Individual Multiwalled Nanotubes," *Phys. Rev. Lett.*, **87**, 215502 (2001).
- <sup>5</sup>N. P. Bansal and D. Zhu, "Thermal Conductivity of Zirconia Alumina Composites," *Ceram. Int.*, **31**, 911–6 (2005).
- <sup>6</sup>K. Balani, S. R. Bakshi, Y. Chen, T. Laha, and A. Agarwal, "Role of Powder Treatment and CNT Dispersion in the Fracture Toughening of Plasma-Sprayed Aluminum Oxide–Carbon Nanotube Ceramic Nanocomposite," *J. NanoSci. Nanotech.*, (2007) doi: 10.1166/jnn.2007.851.
- <sup>7</sup>R. D. Cowan, "Pulse Method of Measuring Thermal Diffusivity at High Temperatures," *J. Appl. Phys.*, **34**, 926–7 (1963).
- <sup>8</sup>FactSage 5.2, <http://www.factsage.com/> (GTT Technologies, Kaiserstr. 100, 52134 Herzogenrath, Germany, 2003)
- <sup>9</sup>C. Masarapu, L. L. Henry, and B. Wei, "Specific Heat of Aligned Multiwalled Carbon Nanotubes," *Nanotechnology*, **16**, 1490–4 (2005).
- <sup>10</sup>C. Poulier, D. S. Smith, and J. Absi, "Thermal Conductivity of Pressed Powder Compacts: Tin Oxide and Alumina," *J. Eur. Ceram. Soc.*, **27**, 475–8 (2007).
- <sup>11</sup>H.-S. Yang, G.-R. Bai, L. J. Thompson, and J. A. Eastman, "Interfacial Thermal Resistance in Nanocrystalline Yttria Stabilized Zirconia," *Acta Mater.*, **50**, 2309–17 (2002).
- <sup>12</sup>S. K. Rhee, "Porosity-Thermal Conductivity Relations Correlations for Ceramic Materials," *Mater. Sci. Eng.*, **20**, 89–93 (1975).
- <sup>13</sup>J. Francl and W. D. Kingery, "Thermal Conductivity: IX, Experimental Investigation of Effect of porosity on Thermal Conductivity," *J. Am. Ceram. Soc.*, **37**, 99–107 (1954).
- <sup>14</sup>J. B. MacEwan, R. L. Stoute, and M. J. F. Notley, "Effect of porosity on the Thermal Conductivity of  $UO_2$ ," *J. Nucl. Mater.*, **24**[1] 109–12 (1967).
- <sup>15</sup>G. Ondracek and B. Schulz, "The Porosity Dependence of Thermal Conductivity of Nuclear Fuels," *J. Nucl. Mater.*, **46**, 253–8 (1973).
- <sup>16</sup>T. A. Taylor, "Thermal Conductivity and Microstructure of Two Thermal Barrier Coatings," *Surf. Coatings Technol.*, **54/55**, 53–7 (1992).
- <sup>17</sup>K. S. Ravichandran, K. An, R. E. Dutton, and S. L. Semiatin, "Thermal Conductivity of Plasma Sprayed Monolithic and Multilayer Coatings of Alumina and Yttria-Stabilized Zirconia," *J. Am. Ceram. Soc.*, **82**, 673–82 (1999).
- <sup>18</sup>R. Landauer, "The Electrical Resistance of Binary Metallic Mixtures," *J. Appl. Phys.*, **21**, 779–84 (1952).
- <sup>19</sup>F. Cernuschi, S. Ahmaniemi, P. Vuoristo, and T. Mantyla, "Modelling of Thermal Conductivity of Porous Materials: Application to Thick Thermal Barrier Coatings," *J. Eur. Ceram. Soc.*, **24**, 2657–67 (2004).
- <sup>20</sup>B. Shafiro and M. Kachanov, "Anisotropic Effective Conductivity of Materials With Nonrandomly Oriented Inclusions of Diverse Ellipsoidal Shapes," *J. Appl. Phys.*, **87**, 8561–9 (2000).
- <sup>21</sup>Z. Wang, A. Kulkarni, S. Deshpande, T. Nakamura, and H. Herman, "Effect of Pores and Interfaces on Effective Properties of Plasma Sprayed Zirconia Coatings," *Acta Mater.*, **51**, 5319–34 (2003).
- <sup>22</sup>T. A. Kulkarni, S. Sampath, A. Goland, and H. Herman, "CMT Studies to Characterize Microstructure-property Correlations in Thermal Sprayed Alumina Deposits," *Scripta Mater.*, **43**, 471–6 (2000).
- <sup>23</sup>R. McPherson, "A Model for Thermal Conductivity of Plasma Sprayed Ceramic Coatings," *Thin Solid Films*, **112**, 89–95 (1984).
- <sup>24</sup>S. U. S. Choi, Z. G. Zhang, W. Yu, F. E. Lockwood, and E. A. Grulke, "Anomalous Thermal Conductivity Enhancement in Nanotube Suspensions," *Appl. Phys. Lett.*, **79**, 2252–4 (2001).
- <sup>25</sup>M. J. Biercuk, M. C. Laguno, M. Radosavljevic, J. K. Hyun, A. T. Johnson, and J. E. Fisher, "Carbon Nanotube Composites for Thermal Management," *Appl. Phys. Lett.*, **80**, 2767–9 (2002).
- <sup>26</sup>R. Sivakumar, S. Guo, T. Nishimura, and Y. Kagawa, "Thermal Conductivity in Multi-Wall Carbon Nanotube/Silica-Based Nanocomposites," *Scripta Mater.*, **56**, 265–8 (2007).
- <sup>27</sup>C.-W. Nan, Z. Shi, and Y. Lin, "A Simple Model of Thermal Conductivity of Nanotube-Based Composites," *Chem. Phys. Lett.*, **375**, 666–9 (2003).
- <sup>28</sup>Q. Z. Xue, "Model for Thermal Conductivity of Carbon Nanotube Based Composites," *Physica B*, **368**, 302–7 (2005).
- <sup>29</sup>C.-W. Nan, G. Liu, Y. Lin, and M. Li, "Interface Effect on Thermal Conductivity of Carbon Nanotube Composites," *Appl. Phys. Lett.*, **85**, 3549–51 (2004).
- <sup>30</sup>S. T. Huxtable, D. G. Cahill, S. Shenogin, L. Xue, R. Ozisik, P. Barone, M. Usrey, M. S. Strano, G. Siddons, M. Shim, and P. Keblinski, "Interfacial Heat Flow in Carbon Nanotube Suspensions," *Nat. Mater.*, **2**, 731–4 (2003).
- <sup>31</sup>N. Shenogina, S. Shenogin, L. Xue, and P. Keblinski, "On the Lack of Thermal Percolation in Carbon Nanotube Composites," *Appl. Phys. Lett.*, **87**, 133106 (2005).
- <sup>32</sup>G.-D. Zhan, J. D. Kuntz, H. Wang, C.-M. Wang, and A. K. Mukherjee, "Anisotropic Thermal Properties of Single-Wall-Carbon-Nanotube-Reinforced Nanoceramics," *Phil. Mag. Lett.*, **84**, 419–23 (2004).
- <sup>33</sup>R. McPherson, "On the Formation of Thermally Sprayed Alumina Coatings," *J. Mater. Sci.*, **15**, 3141–9 (1980).
- <sup>34</sup>J. M. Guilemany, J. Nutting, and M. J. Dougan, "A Transmission Electron Microscopy Study of the Microstructures Present in Alumina Coatings Produced by Plasma Spraying," *J. Thermal Spray Technol.*, **6**, 425–9 (1997). □